Sea Ice CCI+

ESA CCI+ Climate Change Initiative

Phase 1: NEW R&D ON CCI ECVs

Contract number:

4000126449/19/I-NB

CCI+ Sea Ice ECV
SEA ICE CONCENTRATION
END 2 END UNCERTAINTY BUDGET
(E3UB)

Reference: D2.2

Issue: 2.0

Date: 5 October 2020

The Norwegian Meteorological Institute (METNO)
Henrik Mohns Plass 1
N-0313 Oslo
Norway
Phone: + 47 22 96 30 00
Fax: + 47 22 96 30 50
E-Mail: thomas.lavergne@met.no
http://www.met.no

Contract	**Deliverable**
PHASE 1 OF THE CCI+ CLIMATE CHANGE INITIATIVE NEW R&D ON CCI ECVS SEA ICE ECV	D2.2 Sea Ice Concentration End 2 End Uncertainty Budget
CLIENT European Space Agency	**CLIENT REFERENCE** 4000126449/19/I-NB
Revision date: 5 October 2020	**Approval** 22 October 2020

Principal Authors

Rasmus Tonboe, Danish Meteorological Institute
Thomas Lavergne, Norwegian Meteorological Institute

Change Record

Issue	Date	Reason for Change	Author(s)
1.0	29 November 2019	First version	T. Rasmussen, F. Floks, R. Tonboe, T. Lavergne
2.0	5 October 2020	Second version	R. Tonboe, T. Lavergne

Document Approval

Role	Name	Signature
Written by:	R. Tonboe	Rasmus Tonboe
Checked by:	T. Lavergne	
Approved by:	A. M. Trofaier	

Contents

1 INTRODUCTION

1.1 Purpose

This document is the End To End Uncertainty Budget for Sea Ice Concentration in the Sea Ice ECV within CCI+ PHASE 1 - NEW R&D ON CCI ECVs, which is being undertaken by a METNO-led consortium. Its purpose is to give a description of the uncertainty budget provided with the products.

1.2 Scope

The E3UB document describes the main error contributions and their impact on the final sea-ice concentration product. It contains a brief overview of the algorithm itself. More information on the algorithm is available in the Algorithm Theoretical Baseline Document.

1.3 Document Status

This is the second version (Year 2) of the E3UB for Sea Ice Concentration within this project.

1.4 Acronyms and Abbreviations

The table below lists the acronyms and abbreviations used in this volume.

Table 1: Acronyms and Abbreviations. Acronyms for the deliverable items (URD, etc…) and partner institutions (AWI,..) are not repeated.

Acronym	Meaning
AMSR-E / AMSR2	Advanced Microwave Scanning Radiometer (for EOS / #2)
AOGCM	Arctic Ocean General Climate Model
AR5, AR6	WMO IPCC Assessment Report series
ASAR	Advanced Synthetic Aperture Radar
C3S	EU Copernicus Climate Change Service
CCI	Climate Change Initiative
CDR	Climate Data Record
CMEMS	EU Copernicus Marine Environment Monitoring Service
CMIP5, CMIP6	Coupled Model Intercomparison Project series
CMUG	Climate Modelling User Group
CRG	Climate Research Group
CS-2	ESA's CryoSat-2
DEWG	CCI Data Engineering Working Group

EASE grid	Equal-Area Scalable Earth Grid
ECMWF	European Centre for Medium-Range Weather Forecasts
ECV	Essential Climate Variable
ENVISAT	ESA's Environmental Satellite
EO	Earth Observation
ERS	European Remote Sensing Satellite
ESA	European Space Agency
ESMR	Electrically Scanning Microwave Radiometer
EUMETSAT	European Organization for the Exploitation of Meteorological Satellites
FoV (*alt* FOV)	Field-of-View
FY3	Feng Yun 3
FYI	First Year Ice
GCOS	WMO's Global Climate Observing System
GCW	WMO's Global Cryosphere Watch
ICDR	Interim Climate Data Record
IMB	Ice Mass Balance buoy
IPCC	WMO's Intergovernmental Panel on Climate Change
L1b, L2, L3C, ...	Satellite data processing Level (Level-1b, …)
MERIS	MEdium Resolution Imaging Spectrometer
EPS, EPS-SG	EUMETSAT's Polar System, EPS Second Generation
MIZ	Marginal Ice Zone
MODIS	Moderate Resolution Imaging Spectroradiometer
MWI	MicroWave Imager (EPS-SG)
MWRI	Microwave Radiation Imager (Feng Yun 3)
MYI	Multi-Year Ice
NASA	National Aeronautics and Space Administration
NOAA	US National Oceanic and Atmospheric Administration
NSIDC	US National Snow and Ice Data Centre
OE	Optimal Estimation
OIB	Operation Ice Bridge
OSI SAF	EUMETSAT Ocean and Sea Ice Satellite Application Facility
OWF	Open Water Filter
PMR	Passive Microwave Radiometer
PMW	Passive Microwave
RA	Radar Altimeter
RRDP	Round Robin Data Package
SIC	Sea Ice Concentration
SIT	Sea Ice Thickness

SAR	Synthetic Aperture Radar
SIRAL	Synthetic Aperture Radar (SAR) Interferometer Radar Altimeter
SOA	Service Oriented Architecture
SMMR	Scanning Multichannel Microwave Radiometer
SMOS	Soil Moisture and Ocean Salinity
SSM/I	Special Sensor Microwave/Imager
SSMIS	Special Sensor Microwave Imager/Sounder
ULS	Upward Looking Sonar
WMO	World Meteorological Organisation
WSM	Wide Swath Mode

1.5 Executive Summary

All measurements have uncertainties. The brightness temperatures measured onboard the satellite are primarily a function of ice concentration but they are also affected by a number of instrument and geophysical noise sources. We correct for some of these noise sources and that reduces the uncertainty but some sources are difficult to quantify analytically. Therefore, the regionally and temporally varying uncertainties in the sea ice CCI sea ice concentration product are quantified using a forward model and statistical information from the brightness temperatures.

2 HIGH-LEVEL DESCRIPTION OF THE UNCERTAINTY BUDGET

The current SICCI-2 sea ice concentration uncertainty consists of two components: 1) the algorithm uncertainty and 2) the smearing uncertainty. These two components are derived independently, and they are independent so that they can be combined into the total uncertainty. The Algorithm uncertainty is derived from the tie-point variability so that this is linked directly with the estimation of the sea ice concentration. The tie-point variability is a hemispheric quantity which includes instrument noise, emissivity noise, emitting layer temperature noise, cloud liquid water noise and residual noise from imperfections in the NWP data and the RTM. The smearing uncertainty is a representativeness uncertainty related to the fact that information is lost in the imaging process and that the sea ice concentration is not represented on the same resolutions as it is imaged. The smearing uncertainty also includes the satellite foot-print mismatch uncertainty from the use of different frequencies with different spatial resolutions on the ground together. The smearing uncertainty is quantified using a proxy describing the spatial variability of the sea ice concentration. The smearing uncertainty dominates along the ice edge, while it is close to zero in homogeneous sea ice concentration regions or in open water.

The approach to derive and present uncertainties in SICCI-2 is mostly similar to that of the EUMETSAT OSISAF sea ice concentration CDR described in Tonboe et al. (2016), i.e. we make the assumption that the total uncertainty, σ_{total}, is given by two uncertainty components:

$$\sigma^2_{total} = \sigma^2_{algo} + \sigma^2_{smear} \quad \text{eq.1},$$

where σ_{algo} is the inherent uncertainty of the SIC algorithm (algorithm uncertainty) including sensor noise and the residual geophysical noise quantified as variability around the tie-point, and σ_{smear} is the representativeness uncertainty due to resampling from satellite swath to a grid (smearing uncertainty) and footprint mismatch.

What is the algorithm uncertainty? Both the water surface and ice surface emissivity variability and emission and scattering in the atmosphere affect the brightness temperatures and the computed ice concentrations. To reduce the uncertainties due to atmospheric noise, the brightness temperatures are corrected using NWP data for atmospheric water vapour, near-surface air temperature, and open water roughness caused by wind. We are not correcting for cloud liquid water, ice emissivity and effective temperature and the RTM and NWP data are not perfect, therefore there are residual uncertainties. The remaining tiepoint uncertainties are quantified as the tie-point ice concentration standard deviation in regions with open water or 100 % ice.

The derivation of σ_{algo} is to a high extent similar to that described in Tonboe et al. (2016). This term is derived from the accuracy (estimated as statistical variance) of the algorithm to retrieve 0% when applied in regions where we know there is open water and retrieve 100% in regions where we know that there is 100% ice. These two end points are computed as part of the dynamical tie-point estimation procedure. The algorithm uncertainty is therefore directly linked with the sea ice concentration itself. The “v2” SIC algorithm is a “hybrid” algorithm (linearly weighting two other algorithms, each of them optimized for 0% or 100% ice conditions. The algorithm uncertainty of the “hybrid” algorithm is thus also a linear weighting of the algorithm uncertainty (variances) of the two optimized algorithms. The algorithm uncertainty component is computed at Level 2 (swath level sea ice concentrations). Each Level 2 SIC estimate in the data record has an associated σ_{algo} value.

What is the smearing uncertainty? The smearing uncertainty is a representativeness uncertainty. The Tb measurement is the surface and atmospheric emission weighted with a footprint shape function which is both a function of integration time and the antenna gain function. The resampling of the SIC truth to coarser resolution is one aspect of the smearing uncertainty which is increasing as a function of resolution. It needs to be combined with the statistical difference between the truth at a certain grid resolution and the satellite SIC. There is no perfect match between the resampled truth and the satellite SIC but there is a local minimum in the difference between the two at a certain grid resolution. This resolution is coincident with the actual resolution of the satellite SIC.

The perfect match is not achieved because the SIC algorithms are using more than one frequency to minimize the sensitivity to atmospheric noise and different volume scattering magnitude in first- and multiyear ice types. In addition, the higher frequency channels do provide higher spatial resolution SIC. The different frequency Tb's participating in the computation have different spatial resolution leading to a mismatch between footprints. Alternatively, the resolution of the two channels could be resampled to the coarser resolution channel before computing the SIC. This would remove the mismatch. However, the resulting SIC spatial resolution, when the footprints are not resampled is in between the two channels resolution explaining why this practise is maintained: the mixing of resolutions does give higher SIC resolution at the cost of introducing the mismatch uncertainty.

The smearing uncertainty σ_{smear} is difficult to derive analytically and we carry on the approach of Tonboe et al. (2016) to parametrize σ_{smear} as a function of a proxy but it is done differently than in the OSISAF processing.

The uncertainty term σ_{smear} measures the increase of uncertainty due to mismatching spatial dimensions such as when a) the satellite sensor footprint potentially covers a larger or smaller area than that of a target grid cell, or when b) the imaging channels used by the SIC algorithms do not have the same iFoV diameter. Both these effects should have no impact where the sea ice cover is homogeneous within the footprint (fully consolidated sea ice or open water). However, it should be maximum across sharp spatial gradients, typically at the sea ice edge. For the SICCI-2 CDRs we have parameterized σ_{smear} as a function of the $(MAX - MIN)_{3\times3}$ value, that is the difference between the highest and lowest SIC value in a 3x3 grid cells neighborhood around each location in the grid. Specifically:

$$\sigma_{smear} = K \times (MAX - MIN)_{3\times3} \qquad \text{eq.2,}$$

where K is a scalar whose value depends on the iFoV diameter of the instrument channels used for the SIC computation, and the spatial spacing of the target grid. Several other proxies for the local variability of the SIC field were tested (among others the 3x3 standard deviation, the Laplacian, power-to-mean-ratio) and this one was selected for its simplicity and robustness. Values of K were tuned using a radiometer imaging simulator and selected cloud-free scenes of the sea ice MIZ imaged by the Moderate-Resolution Imaging Spectroradiometer (MODIS) as described in Tonboe et al. (2016). A value of K=1 fitted all three SICCI-2 CDRs (Lavergne et al., 2019). In SICCI-2 the value for σ_{smear} is computed as part of the Level 3 chain, after gridding and daily averaging.

The total uncertainty σ_{total} is finally computed using eq 1. In the data files, both the total, the algorithm, and the smearing uncertainty fields are made available.

Importantly, the uncertainties reported in the product files yield for the un-filtered sea-ice concentration values, thus before applying the Open Water Filter (aka Weather Filter). The OWF is a binary flag based on combinations of brightness temperatures. It detects if a Level-2 FoV is most probably ice covered or most probably open water. The OWF is used to detect noise induced by weather, and set the SIC values to 0%. Importantly for the user, the

OWF is applied after the SIC and its uncertainties are computed, and does only impact the SIC field (not the uncertainties).

3 ANALYSIS OF THE UNCERTAINTY BUDGET

The geographical distribution of sea ice concentration uncertainties are shown as a monthly mean for March 2014 in Figure 1. By far the highest uncertainties are found along the ice edge while open water and near 100% ice have relatively low uncertainties. The ice edge uncertainties are dominated by the smearing uncertainty.

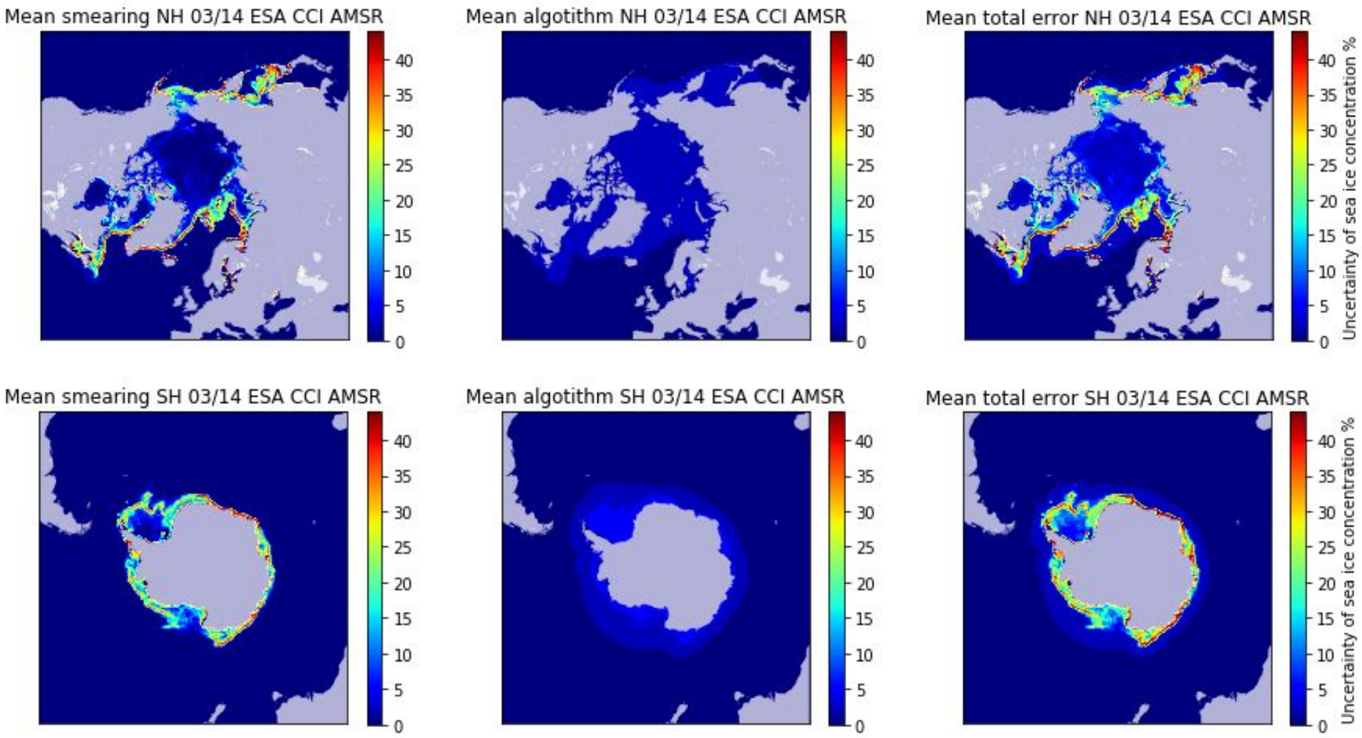

Figure 1: The monthly (March 2014) mean geographical distribution of the SIC uncertainties and its components, the smearing uncertainty (left), the algorithm uncertainty (mid) and the combination of the two, the total uncertainty (right) expressed as one standard deviation in SIC percentage. The upper row is showing the Northern Hemisphere and the lower panel is showing the Southern Hemisphere.

The algorithm uncertainty is shown as a function of the SIC in Figure 2 for the Northern Hemisphere and in Figure 3 for the Southern Hemisphere. The algorithm uncertainty reaches a maximum at intermediate concentrations around 70%. The 70% SIC is where the best-open-water SIC algorithm starts being mixed with the best-ice SIC algorithm. At SIC greater than 90% only the best-ice algorithm is used and at SIC less than 70% only the best-open-water algorithm is used. The mixing between algorithms is done for SIC and uncertainties.

In the lower end of SIC's between 1 and about 15% there are not many SIC values because of the open water filter. The open water filter is constraining open water pixels to 0% SIC according to a set of criterias using the spectral gradient at 19, and 37GHz. Even if a pixel is "caught" in the open water filter it still retains the uncertainty first assigned to it. The open water filter is applied after both SIC and corresponding uncertainty is computed.

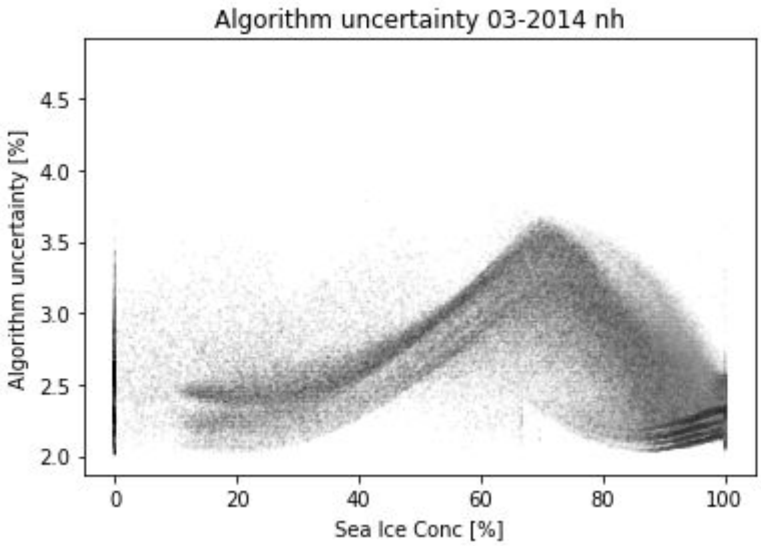

Figure 2: The Northern Hemisphere (March 2014) algorithm uncertainty expressed as one standard deviation in SIC percentage as a function of SIC. The algorithm uncertainty is indeed a function of SIC and the scatter of points is explained by the temporal variability of the tie-point variability.

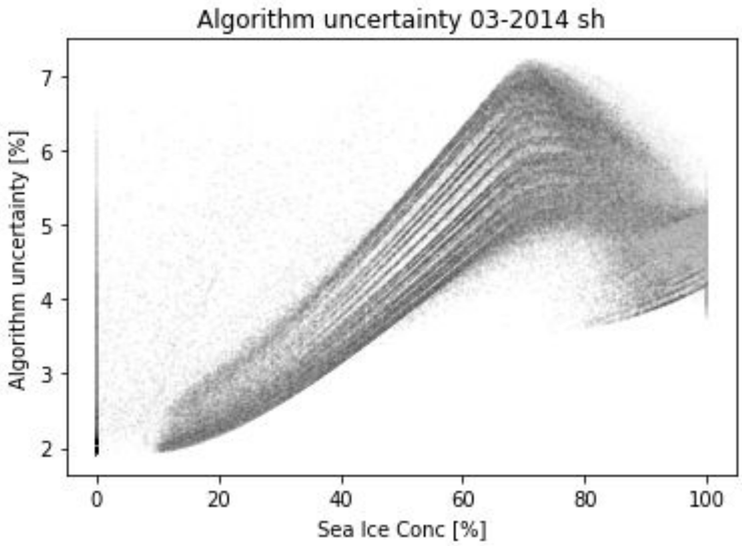

Figure 3: The Southern Hemisphere (March 2014) algorithm uncertainty expressed as one standard deviation in SIC percentage as a function of SIC. The algorithm uncertainty is indeed a function of SIC and the scatter of points is explained by the temporal variability of the tie-point variability. The algorithm uncertainty is higher in summer than in winter explaining why the March algorithm uncertainty is larger over ice on the Southern Hemisphere than on the Northern Hemisphere.

The smearing uncertainty as a function of SIC is shown in Figure 4 for the Northern Hemisphere and in Figure 5 on the Southern Hemisphere.

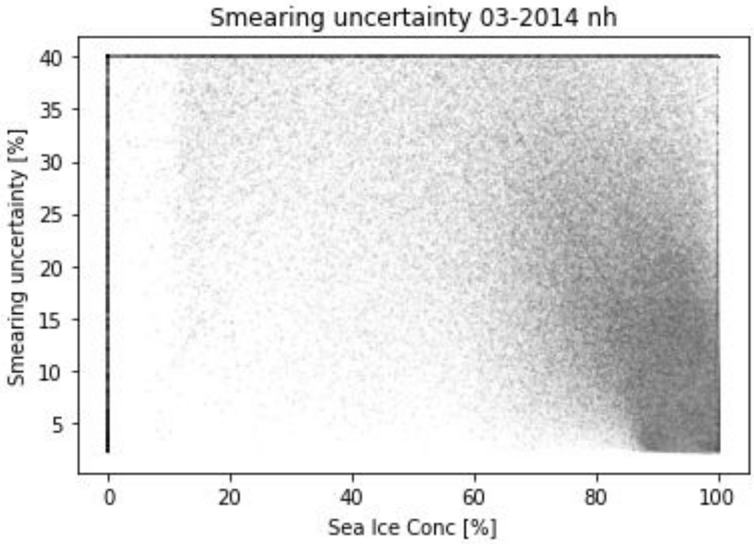

Figure 4: The smearing uncertainty on the Northern Hemisphere (March 2014) as a function of SIC expressed as one standard deviation in SIC percentage. The smearing uncertainty is not a function of SIC but rather a function of SIC local variability. The local SIC variability tends to be higher at intermediate concentration compared to open water and 100% ice.

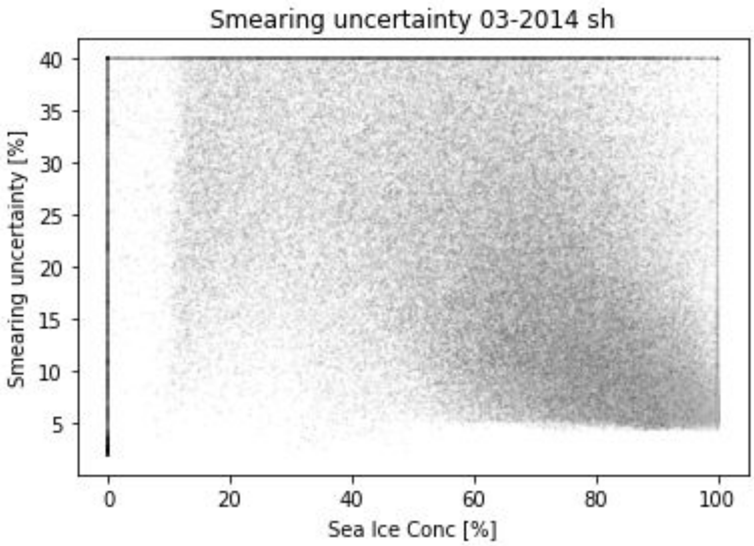

Figure 5: The smearing uncertainty on the Southern Hemisphere (March 2014) as a function of SIC expressed as one standard deviation in SIC percentage. The smearing uncertainty is not a function of SIC but rather a function of SIC local variability. The local SIC variability tends to be higher at intermediate concentration compared to open water and 100% ice.

4 SUMMARY AND CONCLUSIONS

The sea ice concentration uncertainty is computed the combination of two independent components:

1. The algorithm uncertainty which includes instrument noise, emissivity noise, emitting layer temperature noise, cloud liquid water noise and residual noise from imperfections in the NWP data and the RTM.
2. The smearing uncertainty which is a representativeness uncertainty related to the fact that information is lost in the imaging process and that the sea ice concentration is not represented on the same resolutions as it is imaged. The smearing uncertainty also includes the satellite foot-print mismatch uncertainty from the use of different frequencies with different spatial resolutions on the ground together.

Geographically, the smearing uncertainty dominates near the ice edge. The algorithm uncertainty is a function of SIC and reaches a maximum near 70% SIC. The smearing uncertainty is a function of local SIC variability.

5 REFERENCES

Lavergne, T., Sørensen, A. M., Kern, S., Tonboe, R., Notz, D., Aaboe, S., Bell, L., Dybkjær, G., Eastwood, S., Gabarro, C., Heygster, G., Killie, M. A., Brandt Kreiner, M., Lavelle, J., Saldo, R., Sandven, S., and Pedersen, L. T.: Version 2 of the EUMETSAT OSI SAF and ESA CCI sea-ice concentration climate data records, The Cryosphere, 13, 49–78, https://doi.org/10.5194/tc-13-49-2019, 2019.

Tonboe, R. T., Eastwood, S., Lavergne, T., Sørensen, A. M., Rathmann, N., Dybkjær, G., Pedersen, L. T., Høyer, J. L., and Kern, S.: The EUMETSAT sea ice concentration climate data record, The Cryosphere, 10, 2275–2290, https://doi.org/10.5194/tc-10-2275-2016, 2016.